

Hydrodynamics of Topological Defects in Nematic Liquid Crystals

Géza Tóth,¹ Colin Denniston,² and J. M. Yeomans¹

¹*Department of Physics, Theoretical Physics, University of Oxford, 1 Keble Road, Oxford OX1 3NP, United Kingdom*

²*Department of Physics and Astronomy, The Johns Hopkins University, Baltimore, Maryland 21218*
(Received 3 August 2001; published 26 February 2002)

We show that backflow, the coupling between the order parameter and the velocity fields, has a significant effect on the motion of defects in nematic liquid crystals. In particular, the defect speed can depend strongly on the topological strength in two dimensions and on the sense of rotation of the director about the core in three dimensions.

DOI: 10.1103/PhysRevLett.88.105504

PACS numbers: 61.30.Jf, 83.80.Xz

Topological defects arise in all areas of physics from cosmic strings [1] to vortices in superfluid helium [2]. Although the physical systems are very different, many aspects of the observed phenomena match even quantitatively, making it possible to test cosmological predictions experimentally in condensed matter systems [1]. Defects are classified according to their topological strength, and in many cases, the symmetries of the field equations lead to dynamics where defects of opposite topological strength can be mapped into each other. In this Letter, we show an example, of topological line defects in liquid crystals [3], where this symmetry is broken, due to the coupling to an additional field, the flowfield, or to elastic constants that are not equal.

In liquid crystals the topological defects are moving within a liquid and therefore one must expect hydrodynamics to play an important role in their dynamics. In particular, as the defects move, the coupling between the changing director field and the velocity field (so-called backflow) may play a significant part in the motion. Experimental evidence [4] shows that this is indeed the case when a nucleated domain where the director field is horizontal grows in a twist or vertical environment due to the influence of the surfaces or an external electric field. The speed of the domain boundary is found to depend strongly on the local defect configuration.

Previous investigations [5–8] of defect dynamics have either ignored the flow field or taken account of its effect phenomenologically. Here we aim to generalize this work by treating the full hydrodynamic equations of motion for a nematic liquid crystal. We consider the annihilation of a pair of defects of strength $s = \pm 1/2$. We find that backflow can change the speed of defects by up to $\sim 100\%$. Defects of different strength couple to the flow field in different ways. This leads to a dependence of speed on strength which can occur either as a result of the backflow or if the elastic energy is treated beyond a one-elastic constant approximation.

The hydrodynamics of liquid crystals is often well described by the Eriksen-Leslie-Parodi equations of motion, which are written in terms of the director field. However,

these are restricted to an uniaxial order parameter of constant magnitude. Thus they are inadequate to explore the hydrodynamics of topological defects where the magnitude of the order parameter has a steep gradient and becomes biaxial within the core region [9]. Here we consider the more general Beris-Edwards [10] formulation of nemato-hydrodynamics, where the equations of motion are written in terms of a tensor order parameter \mathbf{Q} .

The equilibrium properties of the liquid crystal are described by a Landau–de Gennes free energy density [3]. This comprises a bulk term

$$f_b = \frac{A}{2} \left(1 - \frac{\gamma}{3}\right) Q_{\alpha\beta}^2 - \frac{A\gamma}{3} Q_{\alpha\beta} Q_{\beta\gamma} Q_{\gamma\alpha} + \frac{A\gamma}{4} (Q_{\alpha\beta}^2)^2, \quad (1)$$

which describes a first order transition from the isotropic to the nematic phase at $\gamma = 2.7$, together with an elastic contribution

$$f_d = \frac{L_1}{2} (\partial_\alpha Q_{\beta\gamma})^2 + \frac{L_2}{2} (\partial_\alpha Q_{\alpha\gamma}) (\partial_\beta Q_{\beta\gamma}) + \frac{L_3}{2} Q_{\alpha\beta} (\partial_\alpha Q_{\gamma\epsilon}) (\partial_\beta Q_{\gamma\epsilon}), \quad (2)$$

where the L 's are material specific elastic constants. The Frank expression for the elastic energy, written in terms of the derivatives of the director, can be simply mapped to (2) [10]. A controls the relative magnitude of f_b and f_d . The Greek indices label the Cartesian components of \mathbf{Q} , with the usual sum over repeated indices.

The dynamics of the order parameter is described by the equation

$$(\partial_t + \vec{u} \cdot \nabla) \mathbf{Q} - \mathbf{S}(\mathbf{W}, \mathbf{Q}) = \Gamma \mathbf{H}, \quad (3)$$

where \vec{u} is the bulk fluid velocity and Γ is a collective rotational diffusion constant. The term on the right-hand side of Eq. (3) describes the relaxation of the order parameter towards the minimum of the free energy \mathcal{F}

$$\mathbf{H} = -\frac{\delta \mathcal{F}}{\delta \mathbf{Q}} + (\mathbf{I}/3) \text{Tr} \left\{ \frac{\delta \mathcal{F}}{\delta \mathbf{Q}} \right\}. \quad (4)$$

The term on the left-hand side is

$$\mathbf{S}(\mathbf{W}, \mathbf{Q}) = (\xi \mathbf{D} + \mathbf{\Omega})(\mathbf{Q} + \mathbf{I}/3) + (\mathbf{Q} + \mathbf{I}/3)(\xi \mathbf{D} - \mathbf{\Omega}) - 2\xi(\mathbf{Q} + \mathbf{I}/3) \text{Tr}(\mathbf{QW}), \quad (5)$$

where $\mathbf{D} = (\mathbf{W} + \mathbf{W}^T)/2$ and $\mathbf{\Omega} = (\mathbf{W} - \mathbf{W}^T)/2$ are the symmetric part and the antisymmetric part, respectively, of the velocity gradient tensor $W_{\alpha\beta} = \partial_\beta u_\alpha$. ξ is related to the aspect ratio of the molecules.

The velocity field \vec{u} obeys the continuity equation and a Navier-Stokes equation with a stress tensor generalized to describe the flow of nematic liquid crystals

$$\begin{aligned} \sigma_{\alpha\beta} = & -\rho T \delta_{\alpha\beta} - (\xi - 1) H_{\alpha\gamma} \left(Q_{\gamma\beta} + \frac{1}{3} \delta_{\gamma\beta} \right) - (\xi + 1) \left(Q_{\alpha\gamma} + \frac{1}{3} \delta_{\alpha\gamma} \right) H_{\gamma\beta} \\ & + 2\xi \left(Q_{\alpha\beta} + \frac{1}{3} \delta_{\alpha\beta} \right) Q_{\gamma\epsilon} H_{\gamma\epsilon} - \partial_\beta Q_{\gamma\nu} \frac{\delta \mathcal{F}}{\delta \partial_\alpha Q_{\gamma\nu}}, \end{aligned} \quad (6)$$

where ρ and T are the density and temperature. Notice that the stress (6) depends on the molecular field \mathbf{H} and on \mathbf{Q} . This is the origin of backflow. Details of the equations of motion can be found in Ref. [10]. Equations (1)–(6) were solved numerically using a lattice Boltzmann algorithm described in [11].

Consider a pair of defects of topological strength $s = \pm 1/2$ situated a distance D apart in a nematic liquid crystal, as shown in Fig. 1(a). We consider a two-dimensional cross section of the two line defects, assuming that the order parameter does not change in the perpendicular direction (although the director may point out of this plane). The two defects are topologically distinct only in two dimensions, but even in three dimensions they are separated by an energy barrier for the typical elastic constants we study here.

A phenomenological equation of motion can be written down by assuming that the attractive force between the two defects [3] is counterbalanced by a friction force [7]

$$D \frac{dD}{dt} = \mu_0 \ln^{-1}(D/R_c), \quad (7)$$

where D is the defect separation, R_c is the defect core size, and μ_0 is a constant.

In Ref. [8] the director field and the trajectory of the defects were obtained analytically and the defect velocity was determined as a function of parameters of the medium. (A review of the earlier development of the theory of defect dynamics is also given in [8].) However, this and, as far as we are aware, all other analyses of defect dynamics have ignored backflow. This means that the approach to equilibrium is relaxational, determined entirely by the derivative of the free energy with respect to the order parameter, with the flow playing no role. A further simplification in previous work is that the Frank elastic constants were assumed to be equal.

We can examine relaxational dynamics using a Ginzburg-Landau equation for the director field [12], i.e., Eq. (3) with the velocity set to zero. The Ginzburg-Landau equation with a single elastic constant is invariant under a local coordinate transformation mirroring the director on the x axis (where we define x as the axis connecting the two defects cores). This corresponds to the transformation

$$Q_{xy} \rightarrow -Q_{xy}, \quad Q_{yx} \rightarrow -Q_{yx}. \quad (8)$$

The order parameter fields of the two defects with topological charges $s = \pm 1/2$ transform into each other. Thus approaches based on a simple Ginzburg-Landau equation predict that when the defects move they follow symmetric dynamical trajectories.

Figure 2(a) shows the position of two annihilating topological defects, with topological charge $s = +1/2$ (upper curve) and $s = -1/2$ (lower curve), as a function of time. Figure 2(b) shows the velocities of the defects as the function of their separation D . (See footnote [13] for the simulation parameters.)

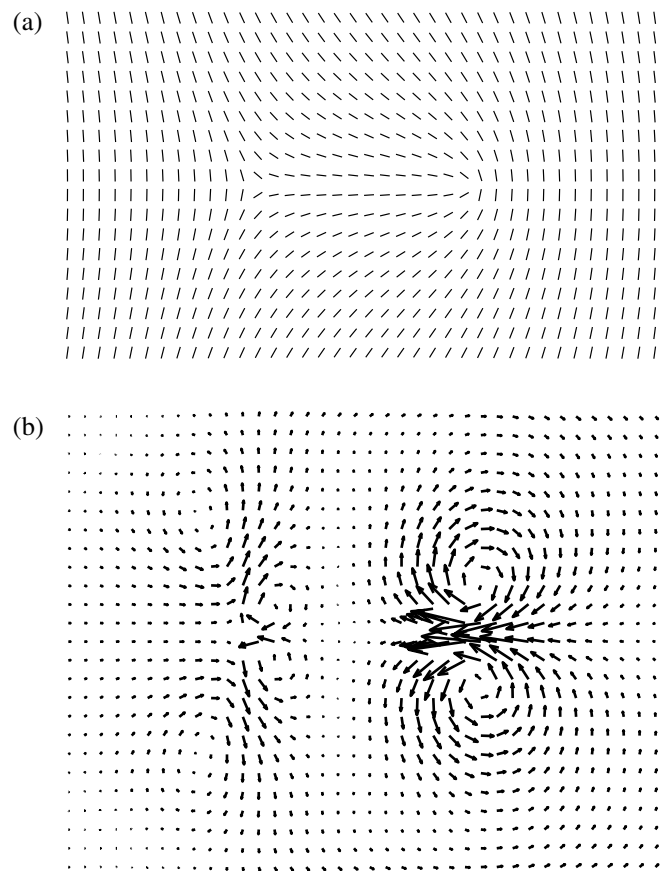


FIG. 1. (a) The director field of two annihilating topological defects with strength $s = \pm 1/2$. (b) Velocity field of the two defects.

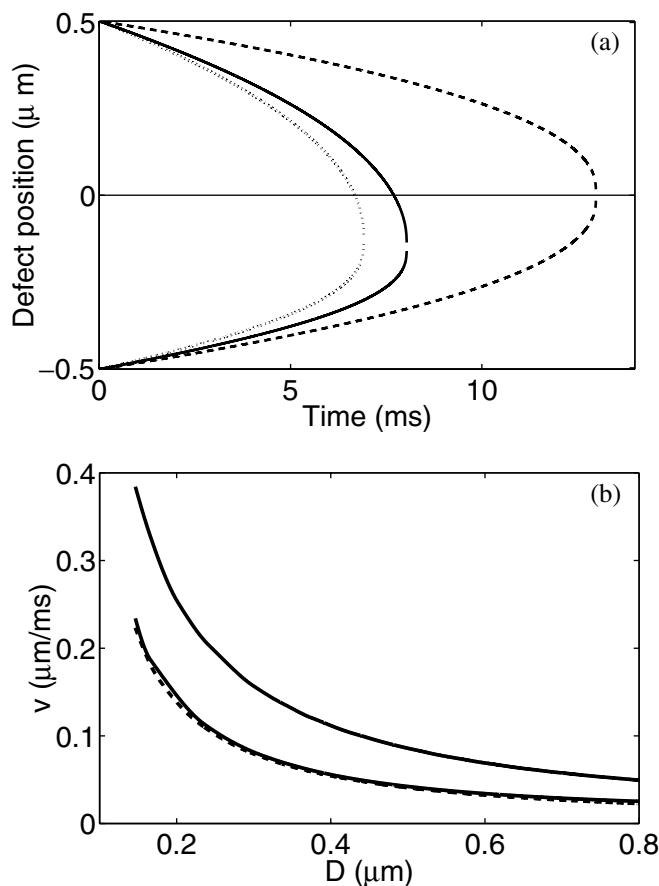


FIG. 2. (a) Positions of the defects as a function of time. Upper (lower) curves are for $s = +1/2(-1/2)$. The different lines correspond to a Ginzburg-Landau model (dashed), the hydrodynamic equations of motion with $\Gamma = 6.25 \text{ Pa}^{-1} \text{ s}^{-1}$ (solid), and with $\Gamma = 7.76 \text{ Pa}^{-1} \text{ s}^{-1}$ (dotted). (b) Defect speed as a function of separation. Upper and lower solid curves: the $s = +1/2$ and $s = -1/2$ defect trajectories with hydrodynamics and $\Gamma = 6.25$; Dashed curve: Ginzburg-Landau model. The $+1/2$ defect is considerably (100%) accelerated for $D > 0.25 \mu\text{m}$ compared to the results of the Ginzburg-Landau model. The speed of the $-1/2$ defect is only slightly affected by the backflow.

Consider first the dashed trajectories. These were obtained with the flow field switched off, the case for which Eq. (3) reduces to a Ginzburg-Landau model. As expected the two defects move with the same speed and annihilate halfway between their initial positions [marked by a horizontal line in Fig. 2(a)]. The results for the Ginzburg-Landau model fit the simple formula (7) for $\mu_0 = 124 \mu\text{m}^2/\text{s}$ and $R_c = 0.0233 \mu\text{m}$ for $D \gtrsim R_c$. Around $D \sim R_c$ the formula overestimates the defect speed.

Consider the effect of the backflow under the transformation of Eq. (8). Examining the stress tensor one can see that the last term in Eq. (6) does not change under the transformation but the off-diagonal elements of the other terms have their sign inverted. This reflects the two sources of backflow in this problem. The first has to do with the defect core. Order is suppressed in the core, which results in an increase in viscosity at the core (the isotropic viscosity α_4 , is proportional to $(1 - q)^2$ where q is the mag-

nitude of the order [10,11]). As a result, the movement of the core induces similar vortices to those produced when a solid cylinder is moved through a fluid. This flow is independent of the sign of the defect, and points into the direction of defect propagation at the core. The second source of backflow comes from the reorientation of the director field away from the core. This flow depends on the sign of the spatial derivative of the director orientation. As a result, these two sources of flow reinforce in one case and partially cancel in the other, thus giving the anisotropy. The flow field around the defects is depicted in Fig. 1(b). A strong velocity vortex pair is formed around the $+1/2$ defect, with the flow pointing in the direction of defect propagation. The flow around the $-1/2$ defect is much weaker, and points opposite to the direction of defect motion.

The solid line in Fig. 2(a) corresponds to a simulation of the full hydrodynamic equations of motion (1)–(6). There is a marked decrease in the time to coalescence. This is primarily because the speed of the $s = +1/2$ defect is increased by $\sim 100\%$ compared to the case without flow for $D \gtrsim 0.25 \mu\text{m}$. The $s = -1/2$ defect is only slightly affected by the backflow; the change in velocity is less than 20%. Because of the speed anisotropy the defects do not meet halfway between their initial positions. For defects initially $1 \mu\text{m}$ apart the displacement of the coalescence point ($\Delta x_1 = 0.149 \mu\text{m}$) is smaller than might be expected from the substantial speed-up of the $s = +1/2$ defect. This is because the relative flow-induced increase in velocity drops dramatically near the defect core ($D \lesssim 0.25 \mu\text{m}$) where the defects are moving the fastest. At these short separations the relaxational dynamics dominates the hydrodynamics.

Changing the various material parameters of the sample will affect the velocity of the defects and their speed anisotropy. We find, as expected, that as the viscosity in the Navier-Stokes equation increases the motion approaches that of the Ginzburg-Landau model. Increasing Γ in (3) increases the speed of relaxation to the minimum of the free energy, thus increasing the speed of the defects. The speed anisotropy, however, decreases because the weight of the free energy relaxation process is increased relative to the hydrodynamics. For example, the dotted curve in Fig. 2(a) corresponds to $\Gamma = 7.76 \text{ Pa}^{-1} \text{ s}^{-1}$ (compared to $\Gamma = 6.25 \text{ Pa}^{-1} \text{ s}^{-1}$ for the solid curve). The displacement of the coalescence point is $\Delta x_2 = 0.128 \mu\text{m} < \Delta x_1$. Decreasing A in the free energy (1) increases the defect size. The defects move faster but the velocity disparity decreases, again because the importance of the relaxational dynamics is increased relative to the hydrodynamics.

The results in Fig. 2 are for a single elastic constant (equal Frank elastic constants or, equivalently, $L_2 = L_3 = 0$). If a more general model for the elasticity is considered, allowing $L_2 \neq 0$ or $L_3 \neq 0$, the invariance of the Ginzburg-Landau equation under the transformation (8) is broken. Therefore one might expect a difference in the velocities of $s = \pm 1/2$ defects even if backflow is not considered.

This is indeed the case. If $L_2 = 0$ and $L_3 < 0$ ($L_3 > 0$) the $s = +1/2$ ($s = -1/2$) defect moves faster. For example, if $L_1 = 8.73$ pN, $L_2 = 0$, and $L_3 = 15.88$ pN [14] a comparison of the velocities $v_{+1/2}, v_{-1/2}$ of the $s = 1/2$ and $s = -1/2$ defects, respectively, gives a speed anisotropy $a_v = (v_{+1/2} - v_{-1/2}) / (\frac{v_{+1/2} + v_{-1/2}}{2}) \sim -13\%$ at a defect separation $D = 0.5 \mu\text{m}$. For comparison, the anisotropy caused by the backflow is $\sim +68\%$. The displacement of the coalescence point is $\Delta x = 0.029 \mu\text{m}$. For most materials $L_3 > 0$ (corresponding to $K_{11} < K_{33}$), leading to a speed anisotropy opposite to that arising from the hydrodynamics.

If $L_2 \neq 0$ and $L_3 = 0$ the velocity anisotropy is very small since for these values of the elastic constants the relaxational Ginzburg-Landau dynamics remains invariant under the mapping (8) in the limit of uniaxiality and constant magnitude of the order parameter [15]. The speed anisotropy is small because these conditions are only relaxed within a defect core. For example, $L_3 = 0$ and $L_2 = 15.88$ pN [16] leads to $|a_v| \lesssim 2\%$.

Anisotropies in the speed of domain walls of up to 50% have been observed in experiments on pi-cell liquid crystal devices where the movement of twist and splay-bend walls is important in mediating the formation of the operating (bend) state from the ground (splay) state. Defects form spontaneously at these walls and preliminary simulations show that backflow effects are responsible for the velocity anisotropy [17]. It is also of interest to investigate the role of defect motion in many other new generation liquid crystal devices. For example, multidomain nematic modes improve viewing angles at the expense of introducing defects into the director profile and understanding the behavior of such defects as the electric field is varied will help control device performance. In zenithal bistable nematic devices switching is between two (meta) stable zero-field states. Switching between the states is mediated by the movement of topological defects [18].

To conclude, we have used a formulation of nematodynamics based on the tensor order parameter to study the hydrodynamics of topological defects in nematic liquid crystals. We find that the coupling between the order parameter field and the flow has a significant effect on defect motion: in particular, it introduces a substantial difference between the velocities of defects of different topological charge. Similar but smaller velocity anisotropies can result from changing the elastic constants.

We would like to thank E. J. Acosta, C. M. Care, J. Dziarmaga, S. Elston, K. Good, O. Kuksenok, S. Lahiri, N. J. Mottram, and T. Sluckin for helpful discussions. We acknowledge the support of Sharp Laboratories of Europe at Oxford. C.D. acknowledges funding from NSF Grant No. 0083286.

[1] N. Turok, Phys. Rev. Lett. **63**, 2625 (1989); A. Pargellis, N. Turok, and B. Yurke, Phys. Rev. Lett. **67**, 1570 (1991).

- [2] D. V. Osborne, Proc. Phys. Soc. London A **63**, 909 (1950).
- [3] P. G. de Gennes and J. Prost, *The Physics of Liquid Crystals* (Clarendon Press, Oxford, 1993), 2nd ed.; M. Doi and S. F. Edwards, *The Theory of Polymer Dynamics* (Clarendon Press, Oxford, 1989).
- [4] E. J. Acosta, M. J. Towler, and H. G. Walton, Liq. Cryst. **27**, 977 (2000).
- [5] C. D. Muzny and N. A. Clark, Phys. Rev. Lett. **68**, 804 (1992); Q. Jiang, J. E. MacLennan, and N. A. Clark, Phys. Rev. E **53**, 6074 (1996).
- [6] L. M. Pismen and B. Y. Rubinstein, Phys. Rev. Lett. **69**, 96 (1992); G. Ryskin and M. Kremenetsky, Phys. Rev. Lett. **67**, 1574 (1991); B. Yurke, A. N. Pargellis, T. Kovács, and D. A. Huse, Phys. Rev. E **47**, 1525 (1993).
- [7] H. Pleiner, Phys. Rev. A **37**, 3986 (1988).
- [8] C. Denniston, Phys. Rev. B **54**, 6272 (1996).
- [9] N. Schopohl and T. J. Sluckin, Phys. Rev. Lett. **59**, 2582 (1987); A. Sonnet, A. Kilian, and S. Hess, Phys. Rev. E **52**, 718 (1995).
- [10] A. N. Beris and B. J. Edwards, *Thermodynamics of Flowing Systems* (Oxford University Press, Oxford, 1994), and references therein.
- [11] C. Denniston, E. Orlandini, and J. M. Yeomans, Europhys. Lett. **52**, 481 (2000); Phys. Rev. E **63**, 056702 (2001).
- [12] A. J. Bray, Adv. Phys. **43**, 357 (1994).
- [13] Simulations were performed on a 350×350 lattice with $A = 1.0$, $L_1 = 0.55$, $L_2 = L_3 = 0$, $\Gamma = 0.625$, $\xi = 0.59$, $\rho = 2.0$, $T = 0.5$, and $\gamma = 3$. Periodic boundary conditions were used in the x direction and free boundaries were used in the y direction. Given suitable pressure, length and time scales these parameters can be mapped to a lattice size $4.4 \mu\text{m} \times 4.4 \mu\text{m}$, $L_1 = 8.73$ pN, $\Gamma = 6.25 \text{ Pa}^{-1} \text{ s}^{-1}$. The Frank elastic constants are $K_{11} = K_{22} = K_{33} = 2L_1 q^2 = 4.37$ pN and Miesowicz viscosities 0.02 Pa s to 0.1 Pa s. The material parameter values chosen are close to those of 4-*n*-pentyl-4'-cyanobiphenyl (5CB).
- [14] $L_1 = 8.73$ pN, $L_2 = 0$, and $L_3 = 15.88$ pN correspond to Frank elastic constants $K_{11} = K_{22} = 3.04$ pN, and $K_{33} = 7.01$ pN.
- [15] If $L_3 = 0$ and the director is confined to the xy plane, the Frank elastic free energy density (assuming uniaxiality and constant magnitude of order) can be written as $f = \frac{\kappa}{2} (\nabla\theta)^2$, where θ is the angle of the director to the horizontal axis and $\kappa = (2L_1 + L_2)q^2$. The dynamics of the medium, $\partial_t \theta = -\Gamma \delta F / \delta \theta = \Gamma \kappa \nabla^2 \theta$, is invariant under mirroring on the x axis. Moreover, a given L_1 and L_2 correspond to the same dynamics as $L'_1 = L_1 + L_2/2$ and $L'_2 = 0$. (Note that there is no speed anisotropy in the latter case with the Ginzburg-Landau model for the tensor order parameter.) For defects this equivalence is only approximate due to the biaxiality and the change in the magnitude of order in the core.
- [16] $L_1 = 8.73$ pN, $L_2 = 15.88$ pN, and $L_3 = 0$ correspond to Frank elastic constants $K_{11} = K_{33} = 8.34$ pN, $K_{22} = 4.37$ pN.
- [17] C. Denniston, G. Tóth, and J. M. Yeomans, J. Stat. Phys. **107**, 187 (2002).
- [18] C. Denniston and J. M. Yeomans, Phys. Rev. Lett. **87**, 275 505 (2001).